Modeling and Analysis of Conventional and Heat-Integrated Distillation Columns

Thomas Bisgaard, Jakob Kjøbsted Huusom, and Jens Abildskov
CAPEC-PROCESS, Department of Chemical and Biochemical Engineering, Technical University of Denmark, Søltofts Plads Building 229, DK-2800 Kgs. Lyngby, Denmark

DOI 10.1002/aic.14970
Published online August 22, 2015 in Wiley Online Library (wileyonlinelibrary.com)

A generic model that can cover diabatic and adiabatic distillation column configurations is presented, with the aim of providing a consistent basis for comparison of alternative distillation column technologies. Both a static and a dynamic formulation of the model, together with a model catalogue consisting of the conventional, the heat-integrated and the mechanical vapor recompression distillation columns are presented. The solution procedure of the model is outlined and illustrated in three case studies. One case study being a benchmark study demonstrating the size of the model and the static properties of two different heat-integrated distillation column (HIDiC) schemes and the mechanical vapor recompression column. The second case study exemplifies the difference between a HIDiC and a conventional distillation column in the composition profiles within a multicomponent separation, whereas the last case study demonstrates the difference in available dynamic models for the HIDiC and the proposed model. © 2015 American Institute of Chemical Engineers *AIChE J*, 61: 4251–4263, 2015
Keywords: heat-integrated distillation column, diabatic, distillation, heat integration, simulation

Introduction

Conventional multistage distillation is the most common unit operation in the chemical industry today.[1] It is frequently referred to as a mature technology; however, alternative intensified and/or heat-integrated configurations have been studied in recent decades with the goal reducing required utility and inventory for a given separation task.

The mechanical vapor recompression column (MVRC) and the heat-integrated distillation column (HIDiC) are considered as promising, related alternatives to the conventional distillation column (CDiC). These configurations are illustrated in Figure 1. In the MVRC, a compressor is introduced to compress the top vapor such that its temperature is raised above the reboiler temperature. This enables the rejected latent heat in the condenser to be utilized in the reboiler thereby lessening the requirement for hot utility during continuous operation. In the HIDiC, gradual condensation occurs along the rectifying section and gradual boil-up occurs along the stripping section as heat is exchanged between the sections. This can be realized by operating the rectifying section at a higher pressure by introducing a compression step above the feed stage. Here we address tray separations, although new variants of the HIDiC concept continue to appear.[2]

In dynamic distillation column simulations, the "constant molar overflow" assumption is widely applied which is used to convert the energy hold-up derivatives into algebraic equations.[3] This assumption has been adopted in the HIDiC model by Liu and Qian,[4] which has been applied for both static and dynamic applications. Their model requires constant pressures in the two column sections and ideal mixtures, but it has found usefulness in particular dynamic simulations and optimization due to the low computational efforts required. To account for pressure dynamics, a more rigorous approach is suggested by Ho et al.[5] in which propagation of pressures through each stage in the column is modeled as having first-order dynamics. Alternatively, the propagation of pressure in a HIDiC can be accounted for by correlating vapor flow rates through pressure gradients between column stages as Wang et al.[6] The model presented in this article has similar pressure dynamics as the latter case. If heat integration is not considered, the proposed model reduces to that of a CDiC as presented by, for example, Gani et al.,[7] Cameron et al.,[8] Ruiz et al.,[9] and Gross et al.[10]

One use of the model is to characterize the performances of the HIDiC and the MVRC that have been discussed in a vast number of publications. However, there is still a need for systematically mapping the choice of superior configuration with respect to selected performance criteria of the mentioned configurations for a given separation. This issue has been addressed by among others,[11–15] and it appears that the economic advantage of either configuration is a function of mixture identity, whereas correlations between optimality and relative volatility have been shown for ideal mixtures. Furthermore, several studies have already proven the operability of the HIDiC by simulation[5,16] and experimentally in bench-scale experiments,[17] but more work has to be done for real industrial applications. Thus, this article presents a generic, first principle model for tray distillation

Correspondence concerning this article should be addressed to J. Abildskov at ja@kt.dtu.dk.

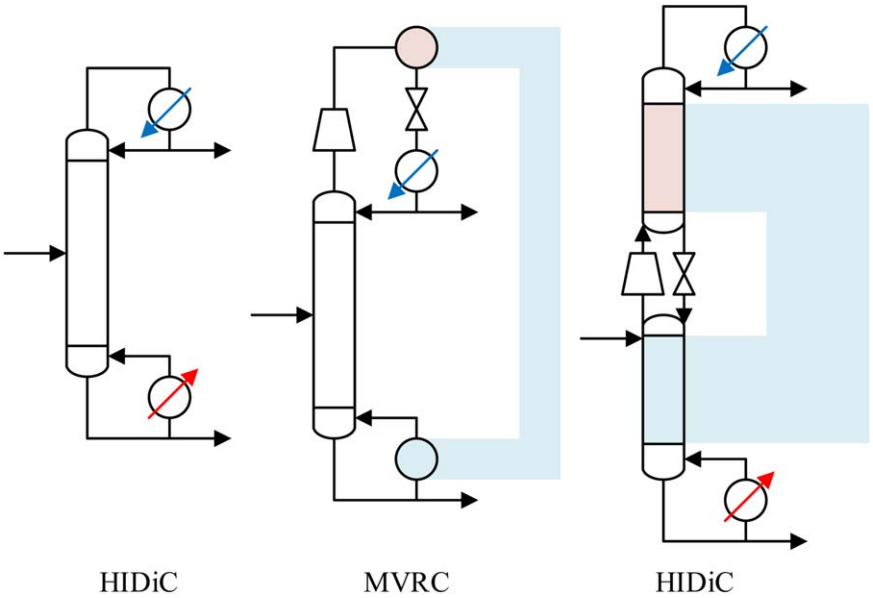

Figure 1. Conceptual illustrations of three configurations indicating similarities.

The CDiC, the MVRC, and the HIDiC[Color figure can be viewed in the online issue, which is available at wileyonlinelibrary.com.]

columns covering the CDiC, the MVRC, and the HIDiC. As a result, it provides a basis for carrying out static and dynamic simulation studies for benchmarking. The model offers a flexibility of considering additional, user-specified heat-integrated configurations due to its generic formulation. We provide a full model documentation and solution procedure for a model covering the conventional and the heat-integrated distillation columns (e.g., the HIDiC and the MVRC). The article is structured as follows: After an introduction, all model equations are presented and described. Third, the model is analyzed, discussed, and the solution procedure is presented. Finally, three application examples are provided as simulation case studies, followed by a discussion and conclusions.

Model

This section provides conservation equations consisting of mass and energy balances for the distillation column, and constitutive equations consisting of vapor-liquid equilibrium, mixture properties, and so forth. A general representation of a column stage is illustrated in Figure 2. All symbols and abbreviations can be found in Notation located in the end. The key features of the model are:

- dynamic mass and energy balances,
- temperature dependence of physical properties,
- liquid phase nonideality by activity coefficient models,
- varying stage pressures, and
- liquid and vapor hydraulics

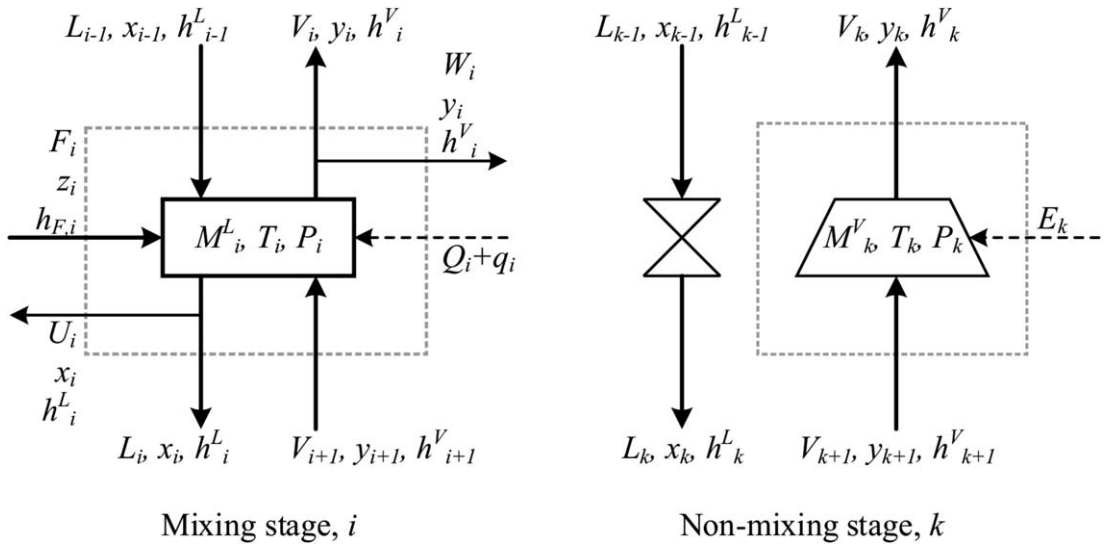

Figure 2. General representation of mixing and nonmixing distillation column stages with nomenclature.

Mass transport is represented by solid lines and energy transport is represented by dashed lines. The gray contours represent control volumes.

Conservation equations

The conservation equations are derived using the control volumes indicated in Figure 2 and cover both mass and energy balances. Individual mass and energy balances are presented for the two-stage classifications. Molar holdups are used as the state variables in the mass balances whereas the energy balances can be converted to temperature derivatives using chain rule algebra. Hence, temperature is preferred as state variables in the energy balances.

Mixing stage

Let $j=1, \ldots, N_C$ denote a component in an N_C-component mixture, and let $i=1,\ldots,N_S$ denote a column stage counted from top including mixing stages (trays, condenser, and reboiler) and nonmixing stages (compressor/valve) as indicated in Figure 2. Conservation of mass of a mixing stage ($i \neq k$) is expressed in moles for each component j

$$\begin{aligned} &d/dt\left(M_{i,j}\right)=L_{i-1}x_{i-1,j}+V_{i+1}y_{i+1,j}+F_i z_{i,j}-(L_i+U_i)x_{i,j} \\ &-(V_i+W_i)y_{i,j}, \quad i=1,...,N_S\backslash\{k\} \end{aligned} \tag{1}$$

$M_{i,j}$ is liquid the molar hold-up, L_i is the liquid flow rate and U_i is the liquid draw flow rate leaving stage i at composition $x_{i,j}$, V_i is the vapor flow rate, and W_i is the vapor draw flow rate leaving stage i at composition $y_{i,j}$, and F_i is the feed flow rate with composition $z_{i,j}$.

Conservation of energy is expressed

$$\begin{aligned} &d/dt(M_{T,i}h_i^L)=L_{i-1}h_{i-1}^L+V_{i+1}h_{i+1}^V+F_i h_{F,i}+Q_i+q_i \\ &-(L_i+U_i)h_i^L-(V_i+W_i)h_i^V, \ i=1,..,N_S\backslash\{k\} \end{aligned} \tag{2}$$

Here $M_{T,i}$ is the total molar hold-up, $h^L{}_i$ is the liquid phase enthalpy, and $h^V{}_i$ is the vapor phase enthalpy, Q_i is the external heat transfer rate, and q_i is the internal heat transfer rate. The left-hand side of Eq. 2 is a simplification of the total energy hold-up by neglecting the vapor hold-up and assuming incompressible liquid[3]

$$d/dt\left(M_{T,i}^L u_i^L+M_{T,i}^V u_i^V\right) \approx d/dt\left(M_{T,i}^L h_i^L\right), \quad M_{T,i}^V \approx 0,\ u_i^L \approx h_i^L \tag{3}$$

where u_i denotes internal energy with superscripts L and V referring to the liquid and the vapor phases, respectively. This assumption is reasonable to the same extent as the ideal gas assumption.

Nonmixing stage

For a nonmixing stage, k, the total hold-up dynamics are neglected. This applies to the valve and the compressor, where the total molar hold-up is assumed constant, leading to the mass balance

$$d/dt\left(M_{k,j}^V\right)=V_k/M_{T,k}(y_{k+1,j}-y_{k,j}), \qquad 2 \le k \le N_S-1 \tag{4}$$

Note that Eq. 4 only applies to the compressor whereas the valve is at steady state. The assignment of k depends on the distillation configuration to be considered and is discussed in Configuration Parameters under Model Framework and Analysis. As a result of assuming constant hold-up, the fast dynamics associated with transient density variations affecting the inlet and outlet flow rates are ignored. Dynamic simulations of a centrifugal compressor[18] support this assumption.

Conservation of energy gives

$$d/dt(u_k^V)=V_k/M_{T,k}\left[h_{k+1}^V-h_k^V+E_k/V_k\right], \quad 2 \le k \le N_S-1 \tag{5}$$

E_k is the power input to the compressor. The compression is assumed dry, that is, no condensation occurs. For vapor phase hold-up, the internal energy must be used which is related to enthalpy through the definition $u=h-Pv$ in which v is the molar volume. One way of considering a nonmixing stage is using a more generic representation of the mass and energy balances as Eqs. 1 and 2 and define the appropriate stream properties for the liquid stream through the valve by steady-state considerations and assuming throttling is isenthalpic. Note that the internal energy is given in Eq. 5, as the vapor phase is considered, which must be accounted for.

Constitutive equations

This section presents a default set of constitutive equations that can be replaced according to application as various pure component (heat capacity, vapor pressure, etc.) and mixture (activity coefficient models) relations are available.

Vapor-liquid equilibrium

Assuming an ideal vapor phase and a negligible contribution from the Poynting correction, the Modified Raoult's law states

$$y_{i,j}=x_{i,j}\gamma_{i,j}P_{i,j}^{sat}/P_i \tag{6}$$

where $\gamma_{i,j}$ is the liquid phase activity coefficient of component j at stage i, $P^{sat}{}_{i,j}$ is the liquid phase saturation pressure, and P_i is the stage pressure. Note that the activity coefficient model should be chosen carefully depending on the system and its prediction of the liquid phase stability should be investigated.[19]

The vapor pressure of component j in liquid on stage i is calculated by the DIPPR 101 correlation

$$P_{i,j}^{sat}=\exp\left[A_j+B_jT_i^{-1}+C_j\ln(T_i)+D_jT_i^{E_j}\right] \tag{7}$$

In which A_j, B_j, C_j, D_j, and E_j are pure component parameters and T_i is the stage i temperature. Finally, the pressure can be calculated by a bubble pressure calculation, derived from Eq. 6

$$P_i=\sum_{j=1}^{N_C}x_{i,j}\gamma_{i,j}P_{i,j}^{sat} \tag{8}$$

Enthalpy

The ideal gas heat capacity form has been adopted from the DIPPR 107 correlation

$$\begin{aligned} c_{P,i,j}^V&=A_j+B_j\left(C_j/\left(T_i\sinh\left(C_j/T_i\right)\right)\right)^2+D_j\left(E_j/\left(T_i\cosh\left(E_j/T_i\right)\right)\right)^2 \\ c_{P,i,j}^L&=c_{P,i,j}^V-d/dT\left(\Delta h_{vap,i,j}\right) \end{aligned} \tag{9}$$

In which A_j, B_j, C_j, D_j, and E_j are pure component parameters. $c_{P,i,j}$ is the constant pressure heat capacity and $\Delta h_{vap,i,j}$ is the heat of vaporization. The ideal gas vapor enthalpy is expressed relative to its value at T_{ref}

$$\begin{aligned} h_{i,j}^V&=h_{ref,j}^{\circ}+\int_{T=T_{ref}}^{T_i}c_{P,i,j}^V dT \\ h_i^V&=\sum_{j=1}^{N_C}y_{i,j}h_{i,j}^V \end{aligned} \tag{10}$$

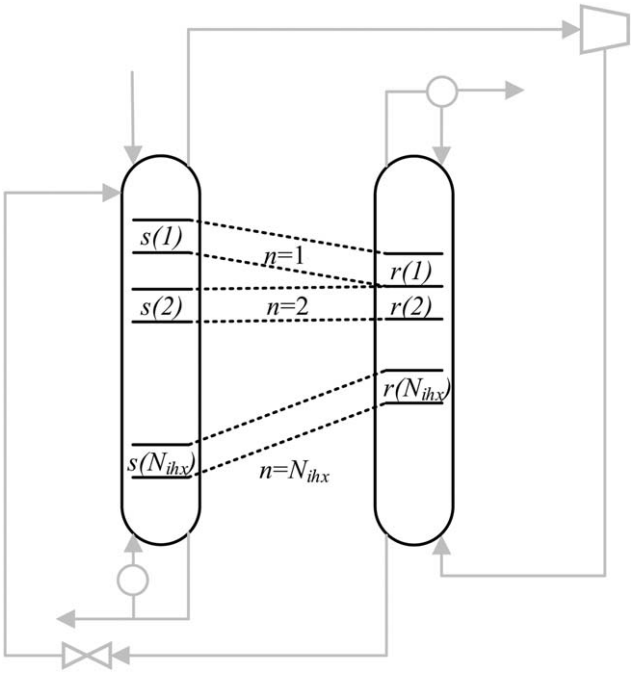

Figure 3. Relation between indices denoting internally heat-integrated stages.

The heat of vaporization of component j is given by the DIPPR 106 correlation

$$\Delta h_{\mathrm{vap},i,j} = A_j\left(1-T_{\mathrm{r},i,j}\right)^{B_j+C_jT_{\mathrm{r},i,j}+D_jT_{\mathrm{r},i,j}^2}$$
$$T_{\mathrm{r},i,j} = T_i/T_{\mathrm{c},j} \tag{11}$$

In which A_j, B_j, C_j, and D_j (third order term is ignored) are pure component parameters while $T_{\mathrm{c},j}$ is the critical temperature of a component and $T_{\mathrm{r},i,j}$ is the reduced temperature. The liquid enthalpy is obtained from following expression

$$h_{i,j}^{\mathrm{L}} = h_{i,j}^{\mathrm{V}} - \Delta h_{\mathrm{vap},i,j}$$
$$h_i^{\mathrm{L}} = \sum_{j=1}^{N_C} x_{i,j}h_{i,j}^{\mathrm{L}} \tag{12}$$

The excess enthalpy contribution of nonideal liquid mixtures has been ignored as models may not be sufficiently accurate and thus little advantage is gained from including the term. The significance of including the excess enthalpy contribution has been investigated by Fredenslund et al.[20] and a deviation in the total flow rates of 3–5% was observed.

Entropy

The entropy, s, of the vapor phase is given by that of an ideal gas

$$s_{i,j}^{\mathrm{V}} = \overset{\circ}{s}_{\mathrm{ref},j} + \int_{T=T_{\mathrm{ref}}}^{T_i}\left(c_{P,i,j}^{\mathrm{V}}/T\right)dT - R\ln\left(P/P^{\mathrm{ref}}\right)$$
$$s_i^{\mathrm{V}} = \sum_{j=1}^{N_C} y_{i,j}s_{i,j}^{\mathrm{V}} - R\sum_{j=1}^{N_C} y_{i,j}\ln y_{i,j} \tag{13}$$

The universal gas constant is denoted by R.

As the stage temperature is equal to the bubble temperature, the liquid entropy is simply

$$s_{i,j}^{\mathrm{L}} = s_{i,j}^{\mathrm{V}} - \Delta h_{\mathrm{vap},i,j}/T_i$$
$$s_i^{\mathrm{L}} = \sum_{j=1}^{N_C} x_{i,j}s_{i,j}^{\mathrm{L}} - R\sum_{j=1}^{N_C} x_{i,j}\ln x_{i,j} \tag{14}$$

The contribution of nonideality to the entropy has been neglected.

Miscellaneous equations

The following definitions are used for respectively the liquid mole fraction and the total stage hold-up

$$x_{i,j} = M_{i,j}/M_{T,i}$$
$$M_{\mathrm{T},i} = \sum_{j=1}^{N_C} M_{i,j} \tag{15}$$

Average molecular weights, MW_i, of the liquid and vapor phases can be calculated from those of the pure components, as follows

$$\mathrm{MW}_i^{\mathrm{L}} = \sum_{j=1}^{N_C} x_{i,j}\mathrm{MW}_j$$
$$\mathrm{MW}_i^{\mathrm{V}} = \sum_{j=1}^{N_C} y_{i,j}\mathrm{MW}_j \tag{16}$$

Pure component liquid density is calculated from the DIPPR 105 correlation

$$\rho_{i,j}^{\mathrm{L}} = \mathrm{MW}_jA_j/B_j^{1+(1-T_i/C_j)^{D_j}} \tag{17}$$

The liquid mixture density, $\rho^{\mathrm{L}}{}_i$, is approximated by the ideal expression by assuming no excess volume

$$\rho_i^{\mathrm{L}} = \mathrm{MW}_i\left(\sum_{j=1}^{N_C} x_{i,j}\mathrm{MW}_{i,j}/\rho_{i,j}^{\mathrm{L}}\right)^{-1} \tag{18}$$

Vapor density can be calculated based on the ideal gas expression

$$\rho_i^{\mathrm{V}} = \mathrm{MW}_i^{\mathrm{V}}P_i/(RT_i) \tag{19}$$

Internal heat transfer

Consider a stage-to-stage HIDiC type pairing with N_{ihx} internally heat-integrated stages. The index $n\in[1;\ N_{\mathrm{ihx}}]$ denotes the coupling of stage *r(n)* in the rectifying section and *s(n)* in the stripping section. For internally heat-integrated stages

$$q_{\mathrm{s}(n)} = U_{\mathrm{ihx}}A_{\mathrm{ihx},n}\left(T_{\mathrm{r}(n)} - T_{\mathrm{s}(n)}\right)$$
$$q_{\mathrm{r}(n)} = -q_{\mathrm{s}(n)} \tag{20}$$
$$q_i = 0, \qquad i \neq n$$

Here U_{ihx} is the overall heat-transfer coefficient and $A_{\mathrm{ihx},n}$ is the internal heat-transfer area. The relations between *r(n)* and *s(n)* and n can be specified as a matrix on the form $N \in Z^{N_{\mathrm{ihx}}\times 2}$ where *r(n)* is the first column element in row n and *s(n)* is the second column element in row n. An illustration of the indices is provided in Figure 3.

Nonmixing stage update

The compressor/valve stages are nonmixing stages. The mass and energy dynamics for the compressor are described in

Eqs. 4 and 5, whereas the throttling is assumed adiabatic and at steady state. Hence the following applies to the liquid phase of a nonmixing stage

$$\begin{aligned} x_{k,j} &= x_{k-1,j} \\ h_k^{\mathrm{L}} &= h_{k-1}^{\mathrm{L}} \\ c_k^{\mathrm{L}} &= c_{k-1}^{\mathrm{L}} \\ \mathrm{MW}_k^{\mathrm{L}} &= \mathrm{MW}_{k-1}^{\mathrm{L}} \\ \rho_k^{\mathrm{L}} &= \rho_{k-1}^{\mathrm{L}} \end{aligned} \tag{21}$$

The pressure of the compressor outlet is related to that of the inlet, by the following simplified expression resulting from an isentropic balance for ideal gases

$$P_k = P_{k+1}\left[\eta_{\mathrm{is}}\left(T_k/T_{k+1}-1\right)+1\right]^{\kappa_k/(\kappa_k-1)} \tag{22}$$

Here η_{is} is the isentropic efficiency of compression, and κ_k is the isentropic expansion factor, which is given by the ratio of constant pressure and constant volume heat capacities. For ideal gasses, the isentropic expansion factor is

$$\kappa_k = c_{\mathrm{P},k}^{\mathrm{V}}/c_{\mathrm{V},k}^{\mathrm{V}} = c_{\mathrm{P},k}^{\mathrm{V}}/\left(c_{\mathrm{P},k}^{\mathrm{V}}-R\right) \tag{23}$$

As the heat capacities in the derivation of Eqs. 22 and 23 are assumed constant, a mean heat capacity,[19] based on steady-state column temperatures, can be used in Eq. 23

$$\langle C_{\mathrm{P}}^{\mathrm{V}}\rangle = \int_{T=T_{k+1}}^{T_k} C_{\mathrm{P}}^{\mathrm{V}}\,dT/(T_k-T_{k+1}) \tag{24}$$

Tray hydraulics

It is desired to express the liquid and vapor flow rates as functions of state variables. In a tray column, liquid is entering a tray from the downcomer and leaving by flowing over the weir. Furthermore, vapor enters a tray as bubbles from the bottom of the tray and rises through the liquid where it exchanges matter and energy. From the vapor phase, a flow, caused by a pressure gradient, leaves the tray into the above tray. Liquid flow can be described by the Francis weir formula in which the amount of liquid over a weir is proportional to the volumetric, liquid flow rate leaving the weir to the power of 2/3,[21] hence

$$\begin{aligned} L_i &= \begin{cases} C_i^{\mathrm{L}}\rho_i^{\mathrm{L}}H_{\mathrm{oW},i}^{3/2}/\mathrm{MW}_i^{\mathrm{L}}, & H_{\mathrm{oW},i} > 0 \\ 0, & H_{\mathrm{oW},i} \le 0 \end{cases} \\ H_{\mathrm{oW},i} &= H_{\mathrm{cl},i} - H_{\mathrm{W}} \\ h_{\mathrm{cl},i} &= M_{\mathrm{T},i}\mathrm{MW}_i^{\mathrm{L}}/\left(\rho_i^{\mathrm{L}}\mathrm{A}_{\mathrm{t},i}\right) \end{aligned} \tag{25}$$

Here $C^{\mathrm{L}}{}_i$ is a constant depending on the liquid loading of the individual trays. $A_{\mathrm{t},i}$ is the active area of tray covered by the liquid phase, H_{W} is the weir height, $H_{\mathrm{cl},i}$ is the clear liquid height (froth ignored), and $H_{\mathrm{oW},i}$ is the liquid height above the weir. Both $A_{\mathrm{t},i}$ and H_{W} are dimensional parameters of the column internals.

The vapor flow through perforated plates can be described as done by Kolodzie and van Winkle.[22] In this work, the volumetric flow rate is simplified to be proportional to the square root of the pressure gradient in terms of liquid height

$$\begin{aligned} V_i &= C_i^{\mathrm{V}}\left(\rho_i^{\mathrm{V}}\right)^{0.5}\left(\Delta P_i - \Delta P_{s,i-1}\right)^{0.5}/\mathrm{MW}_i^{\mathrm{V}} \\ \Delta P_i &= P_i - P_{i-1} \\ \Delta P_{\mathrm{s},i-1} &= \rho_{i-1}^{\mathrm{L}} g h_{\mathrm{cl},i-1} \end{aligned} \tag{26}$$

where $C^{\mathrm{V}}{}_i$ is a constant depending on the vapor loading of the individual trays. g is the gravitational acceleration and $\Delta P_{\mathrm{s},i}$ is the hydrostatic pressure drop due to the liquid height, $h_{\mathrm{cl},i}$, provided in Eq. 25.

Performance indicators

Below we define a set of performance indicators with expressions for evaluating these. Traditionally, energy consumption has been a key indicator when comparing HIDiC and CDiC, but economic indicators are critical to evaluate market potential. Even though these are not parts of the model, we will show how to integrate these with the model for comparative studies.

Second-law efficiency

The second-law efficiency, $\eta_{2\mathrm{nd}}$, provides insights into the column energy efficiency and is given by[23]

$$\begin{aligned} \eta_{2\mathrm{nd}} &= W_{\min}/\left(W_{\mathrm{lost}}+W_{\min}\right) \\ W_{\min} &= \sum_{i=1}^{N_{\mathrm{S}}}\left(U_i b_i^{\mathrm{L}}|_{T=T_\sigma} + W_i b_i^{\mathrm{V}}|_{T=T_\sigma} - F_i b_{F,i}|_{T=T_\sigma}\right) \\ W_{\mathrm{lost}} &= \sum_{i=1}^{N_{\mathrm{S}}}\left(U_i b_i^{\mathrm{L}} + W_i b_i^{\mathrm{V}} - F_i b_{\mathrm{F},i} + Q_i\left(1-T_\sigma/T_{\mathrm{s},i}\right)+E_i\right) \\ b_i^{\mathrm{L}} &= h_i^{\mathrm{L}} - T_\sigma s_i^{\mathrm{L}} \\ b_i^{\mathrm{V}} &= h_i^{\mathrm{V}} - T_\sigma s_i^{\mathrm{V}} \\ b_{\mathrm{F},i} &= h_{\mathrm{F},i} - T_\sigma s_{\mathrm{F},i} \end{aligned} \tag{27}$$

where $W_{\min}$ is the minimum, isothermal work, W_{lost} is the lost work, and b_i is the availability function. T_σ is the temperature of the surroundings and $T_{\mathrm{s},i}$ is the temperature of the energy sink or source. The internal heat transfer rate, q_i, does not appear in Eq. 27 and hence the distinguishing from Q_i.

Capital expenditures

One method for estimation of the capital expenditures (CAPEX) is the Guthrie's Modular Method as described by, for example, Biegler et al.[24] This method reflects the median of equipment cost data, which have deviations of about 20% for some units. The CAPEX calculation consists of the summation of costs of updated bare module costs (UMC) of modules corresponding to vessels, trays, heat exchangers, and compressors (see Table 1)

$$\mathrm{CAPEX} = \sum_{f\ \mathrm{modules}} \mathrm{UMC}_f \tag{28}$$

The UMC includes material and pressure correction factors and update factors. The annual index of the chemical engineering plant cost index is taken from Chemical Engineering Plant Cost Index (CE PCI)[25] and the value from 2012 is 584.6. The contributions in terms of bare module costs, *BC*, for a distillation column are (units omitted in equations)

Table 1. Relation Between Distillation Column Modules and Guthrie Modules

Distillation Equipment	Guthrie Module	Comment
Column tower	Horizontal vessel	Heat integrated configurations are priced as consisting of one tower having a constant diameter based on the stage with the largest diameter. The tower height includes extra feed space, disengagement space, and skirt height (totals 20% of total tray stack height). In this way, the HIDiC cost is always overestimated in any arrangement (e.g., concentric).
	Trays	Heat integrated configurations are priced as consisting of one tray stack having the column diameter described for the horizontal vessel.
Condenser	Heat exchanger	Fixing the maximum temperature change of cooling water, $\Delta T_{\text{water,max}}$, inlet temperature $T_{\text{water,in}}$, and the overall heat-transfer coefficient, U_{cnd}, the required heat exchange area can be calculated.
Reboiler	Heat exchanger	Fixing the steam temperature $T_{\text{steam,in}}$, and the overall heat-transfer coefficient, U_{rbl}, the required heat exchange area can be calculated.
Side heat exchangers	Heat exchanger	As condenser or reboiler based on direction of transferred heat.
Pair of internally heat integrated stages	Heat exchanger	Here simple U-tube heat exchangers are used to represent thermal connection of stages despite any internal or external arrangement.
Compressor	Compressor	Centrifugal/motor type compressor is chosen since it is suitable for high capacities and compression ratios up to five.

$$\begin{aligned} \text{BC}_{\text{cln}} &= 963 l^{0.81} d^{1.05} + 125 l^{0.97} d^{1.45} \\ \text{BC}_{\text{hex}} &= 477 A^{0.65} \\ \text{BC}_{\text{cpr}} &= 831 E^{0.77} \end{aligned} \tag{29}$$

with l and d being the column height and diameter in m, respectively, and A for the heat exchangers is the area in m^2, and E for the compressor is the duty in kW. The BC is in \$(USD). Calculating the UMC_i from BC_i requires parameters, which are listed in Biegler et al.[24]

Operation expenditures

The OPEX estimation procedure of a distillation column considers only the utilities. Hence, the OPEX is a summation of all utilities weighted by their prices. The utilities are cold (cooling water), and hot (steam) and electricity

$$\text{OPEX} = \sum_i m_{cold,i} S_{\text{cold},i} + \sum_i m_{\text{hot},i} S_{\text{hot},i} + S_{\text{electricity}} \sum_i E_i \tag{30}$$

The unit of utility prices, S, can be \$ per mass for cold and hot utilities and \$/kWh for electricity. Indices are given on cold and hot utility prices since these can exist in different qualities, for example, low-pressure (LP) steam or high-pressure steam. The mass flow rates, m, can be calculated from the corresponding duties using the assumptions listed in Table 1

$$\begin{aligned} Q_i > 0: \quad & m_{\text{cold},i} = 0 \\ & m_{hot,i} = Q_i \text{MW}_{\text{water}} / \Delta h_{\text{vap,water},i} \\ Q_i < 0: \quad & m_{cold,i} = -Q_i \text{MW}_{\text{water}} / \left(C_{\text{P,water}} \Delta T_{\text{water,max}} \right) \\ & m_{hot,i} = 0 \end{aligned} \tag{31}$$

Here $\Delta T_{\text{water,max}}$ is the maximum temperature change in cooling water satisfying $\Delta T_{\text{water,max}} < T_i - T_{\text{water},i}$, where T_i is the stage where heat is removed with cooling water fed at temperature $T_{\text{water},i}$.

Model Framework and Analysis

The model framework is summarized in Figure 4 illustrating its capability of performing steady-state evaluation and dynamic evaluation of various configurations. The figure illustrates the progress of the steps for implementation depending on the purpose, that is, static or dynamic. Steps 1–2 are conventional steps for separation by distillation where step 3 requires user input for specifying the particular configuration of interest. This is addressed in more details in Configuration Parameters. In step 4, a column design must be selected that

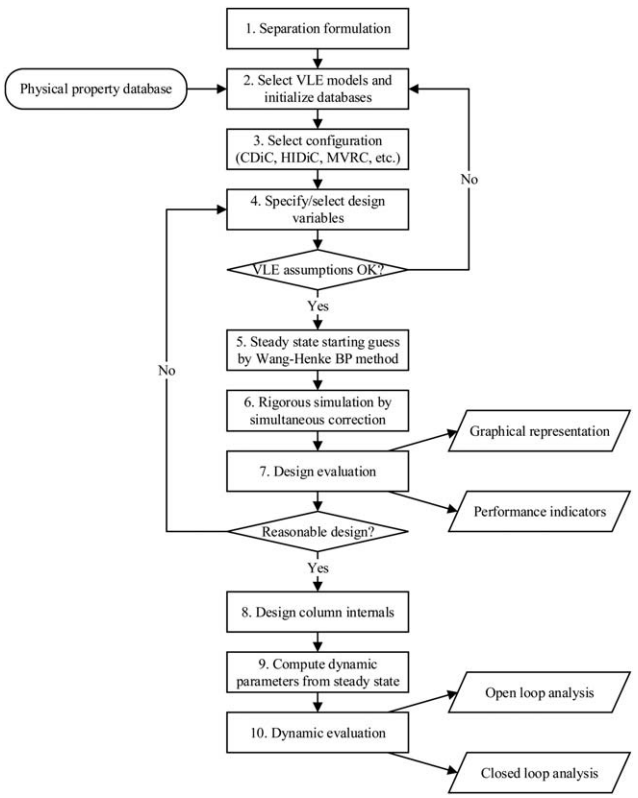

Figure 4. Model framework providing overview of the workflow required in different studies.

Table 2. Model Characterization of the Three Configurations

Position	Set size	Index	Index range		
			CDiC	MVRC	HIDiC
Compressor/valve	N_{cpr}	k	–	2	$2 \le k \le N_F - 1$
Heat-integrated stages in rectifying section	N_{ihx}	r	–	1	$2 \le r \le N_F - 1,\ r \ne k$
Heat-integrated stages in stripping section	N_{ihx}	s	–	N_S	$N_F \le s \le N_S - 1,\ s \ne k$

See Figure 3 for explanation of indices.

is, the design degrees of freedom (see Proposed Specifications) must be specified. No simple short-cut method exists but design studies do exist and proposals continues to appear.[12,26,27] Steps 5–6 results in a steady state where step 5 significantly improves the convergence rate by providing an initial guess by solving the equations sequentially, whereas all equations are solved simultaneously in step 6. The subsection Performance Indicators under Model provides a basis for evaluating a distillation column design for step 7, where graphical representations such as an xy-diagram and/or xy-enthalpy diagram can be useful for evaluating the simulation results. If dynamic simulations are required one has to proceed to steps 8–10, beginning in step 8 with fixing hydraulic parameters appearing in Eqs. 25 and 26 covering, for example, active tray area and weir height. These parameters are converted to the proportionality constants in the same equations in step 9 such that dynamic simulations can be carried out in step 10. The implementation procedure is provided at the end of this section.

Configuration parameters

The proposed model framework offers a great flexibility with respect to selection of distillation configurations, and ultimately a generalized foundation for comparisons. The three configurations introduced in Figure 1 can be represented using the guidelines of parameter selection in Table 2. Take for example the MVRC for which the position of the compressor/valve stage must be at stage 2 whereas for the HIDiC it must be in the rectifying section, that is, above the feed stage. The framework furthermore enables studies, which incorporate for example additional compressors to cope with separations having complex column temperature profiles or higher energy utilization.

Proposed specifications

A degree-of-freedom analysis is summarized in Table 3. An analysis is presented for both the steady state and the dynamic model. The proposed steady-state degrees of freedom are based on CDiCs, and the proposed degrees of freedom for the dynamic model is identified by counting the number of independent material and energy streams that can be manipulated. As a result of considering the dynamics of the compressor, this model has an additional operational degree of freedom as the one proposed by Ho et al.,[5] which is the compressor duty.

Dynamic parameters

The dynamic model contains additional parameters compared to simpler approaches.[4] This increases model flexibility at the cost of an increased number of parameters that have physical meaning and therefore are bounded within reasonable/realistic limits. A list of recommendations for fixing these parameters is compiled in Table 4. For liquid and vapor hydraulics, it is suggested to specify driving forces.

The steady state is determined by extending the Wang–Henke boiling point method as other authors.[28,29] This steady state is, however, only used as an initial guess for a simultaneous solution formulation.

Implementation

The calculation sequence of the model equations is based on the framework provided by Gani et al.[7] The set of model equations is decomposed into smaller subsets that can be solved sequentially and individually from one another as illustrated in Figure 5. In addition, the dynamic model can be solved as a system of coupled, ordinary differential equations if vapors are considered ideal gases and when deviation from nonideality of the liquid phase is described as a function of liquid phase state variables temperature and composition. When nonideality of the vapor phase is the case, a differential-algebraic equation solver must be used which increases the complexity of the solution procedure. One might argue that the HIDiC has a main application in the low-to-medium pressure range since the pressure elevation is often minimized to reduce operational electricity costs and CAPEX associated with compression unit.

Case Studies: Application to Separation of Aromatics

This chapter demonstrates the application range of the presented model through three examples covering steady-state benchmarking of binary and multicomponent systems, and a dynamic study. The benzene-toluene separation forms our representative binary separation, since this has been widely applied in HIDiC studies in the literature. The following sections will sequentially explain the link between the model and the framework presented in Figure 4. The full model is implemented in a MATLAB® environment.

Steady-state benchmarking

Consider the separation of 83.3 mol/s equimolar mixture of benzene/toluene consisting of 50% vapor. An optimal CDiC design based on minimum total annualized cost (TAC) was obtained by incrementally decreasing the reflux to minimum reflux ratio for obtaining the required number of stages using

Table 3. Proposed Specifications Provided All Feed Specifications

	Stage	Condenser	Reboiler	Compressor/Valve
Design	*P, U, W, Q,* Internal heat transfer	Component spec., *P*	Component spec., *P*	*P*
Operation	*U, W, Q*	*L, U, Q*	*U, Q*	*E*

Table 4. Recommendation for Selection of Dynamic Column Design Parameters

Unknown Variable	Appearing in Eqs.	Number of Appearance	Recommended Constraint
C^{V}_{i}	26	$N_S - N_{cnd} - N_{cpr}$	Fix plate pressure drop ΔP_i (e.g., 700 Pa)
C^{L}_{i}	25	$N_S - N_{rbl} - N_{cnd} - N_{cpr}$	Fix liquid height over weir, H_{oW} (e.g., 20% of weir height)
$M_{T,i}$ (reboiler and condenser)	1,2	$N_{rbl} + N_{cnd}$	Fix time constant, $\tau_{acc,i}$, defined as total holdup divided by steady-state throughput (e.g., 5 min)
$A_{t,i}$	25	$N_S - N_{rbl} - N_{cnd} - N_{cpr}$	Use conventional column sizing method
$M_{T,k}$	4,5	N_{cpr}	Fix time constant, $\tau_{cpr,k}$, defined as total holdup divided by throughput (in the order of seconds, see Jiang et al.[18])

the Ponchon-Savarit algorithm.[30] A 42 stages column was obtained including the condenser and the reboiler.

The CDiC design was used as a starting point for the MVRC, by allowing heat-integration between the condenser and reboiler and adding a compression stage thereby obtaining in total 43 stages. Thus $r=1$, $s=43$, and $k=2$ according to Table 2. The heat exchange area and compression ratio were chosen such that no reboiler duty was required and heat transfer occurs at 5 K. In addition, 550 kW of energy was removed from stage 3 for bringing the throttled liquid to its bubble point to avoid excessive compressor duty. The HIDiC design was carried out by heat-integrating all stages excluding condenser, reboiler and compressor stages, and, similar to the MVRC, defining a uniform heat exchange area per stage and compression ratio such that no reboiler duty was required and the minimum temperature difference among all stages was 5 K. Finally, an additional HIDiC configuration referred to as the SIHIDiC (Simplified Ideal HIDiC) is simulated. The number of stages and the thermal coupling is adopted from Chen et al.[31] leading to a column with 15 stages in the rectifying and 19 stages in the stripping section, where only three stages are thermally coupled (#2,#3,#12 with #22,#34,#36, respectively) as a means to reduce overall investment costs. Because of different models and feed flow rates, the compression ratio and heat exchange areas have been chosen differently: The compression ratio is selected similar to that of the HIDiC and heat exchange areas proportional to those of Chen et al. are selected. In addition, the SIHIDiC operates at steady state without external reflux and thus it was found that 404 kW energy must be removed at the feed stage.

All operating conditions and simulation results are listed in Table 5. In this example, following utility prices are used: Electricity 0.14 \$/kWh, LP steam $23.55 \cdot 10^{-3}$ \$/kg, and cooling water $0.080 \cdot 10^{-3}$ \$/kg based on estimates using the correlations by Ulrich and Vasudevan.[32] A conservative estimate of the overall heat-transfer coefficient of 0.6 kW K^{-1} m^{-2} was adopted,[3] which is reasonable considering the experimentally obtained range of 0.7–1.5 kW K^{-1} m^{-2} by de Rijke.[33] A compressor efficiency of 72% was assumed.

Ideal vapor and liquid phases are considered in this simulation. The starting guess of the unknown variables for all configurations is refined using the Wang–Henke bubble point method. Hence, the characteristics of internal heat transfer for the HIDiC besides conventional information as feed characteristics and distillate flow rate and reflux ratio are the only required information. The convergence criteria in this work consists of both tear variables, that is, changes in vapor flows and temperatures. A convergence tolerance of 10^{-8} has been used. For the provided HIDiC design, the method converges in 81 iterations based on a simple initialization of tear variables.[1] The model results in 281 static model equations for the HIDiC, which are solved using a suitable solver to obtain the steady state.

The results reported in Table 5 contain key performance indicators for rigorous distillation column simulations of the four configurations. Even though in practice economics is expected to be the most critical factor, the increasing attention

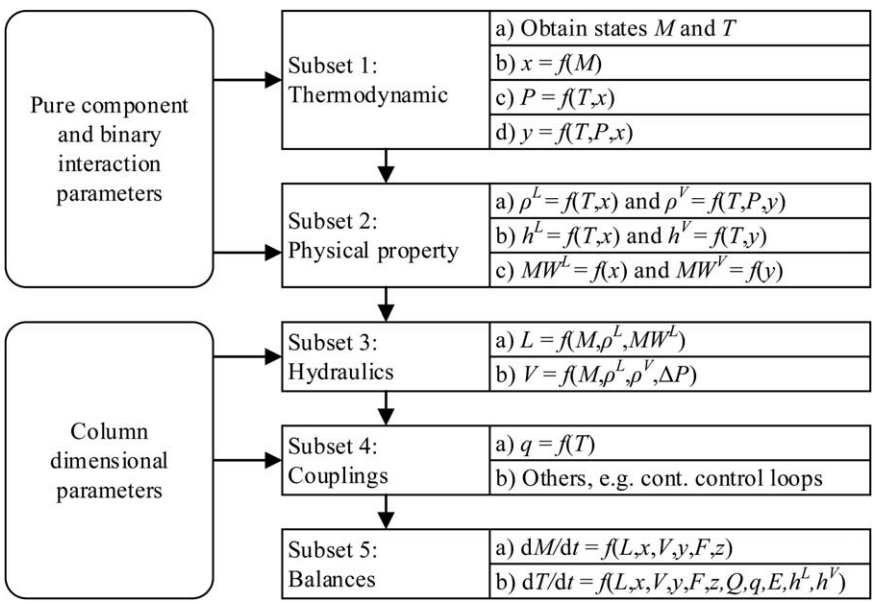

Figure 5. Implementation sequence to obtain a system of ordinary differential equations.

Table 5. Comparison of Three Distillation Configurations in Terms of Performance Indicators

	CDiC	MVRC	HIDiC	SIHIDiC
Stages, -	2 + 20 + 20	3 + 20 + 20	3 + 26 + 26	3 + 15 + 19
Compression ratio, -	1	2.95	2.40	2.76
Heat exchange area of integrated stage(s), m^2	0	826	29.1	177/180/174
Column area, m^2	3.1	3.8	3.9	3.7
Cooling duty, kW	3739	1458	1600	1594
Heating duty, kW	2473	0	0	0
Electricity consumption, kW	0	659	732	783
Second-law efficiency, %	7	16	14	14
Water consumption, 10^9 kg/yr	5.1	2.0	2.2	2.2
CAPEX, 10^6 $	0.84	3.60	4.58	3.86
OPEX, 10^6 $/yr	1.17	0.89	0.99	1.04
TAC (10 year lifetime), 10^6 $/yr	1.2	1.2	1.5	1.4
Payback period, yr	Reference	10	20	23

The feed has a vapor fraction of 0.50, is equimolar mixture of benzene/toluene and is fed at a rate of 83.3 mol/s. A tray pressure drop of 0.35 kPa is assumed.

on environmental aspects such as water and energy efficiency makes such factors become increasingly important. Hence, evaluating the best alternative requires considerations on multiple aspects and the best solution might be a tradeoff:

- Sustainability: Energy consumption, second-law efficiency, water consumption
- Economics: Capital expenditures, operation expenditures
- Practical: For example, hydraulic feasibility indicator[26]

This example clearly illustrates the complexity of benchmarking the proposed configurations: The CDiC and the MVRC are the preferred configurations w.r.t. TAC over the HIDiC and the SIHIDiC. For the HIDiCs, it is not clear whether the increased CAPEX and complexity of design and operation can justify the relatively low reductions in OPEX when taking into account uncertainties of economic models and data. The observation that the MVRC is the economically preferred configuration in terms of TAC is in good agreement with the conclusions from similar studies,[11,12] who claim that the simpler MVRC as a rule of thumb has better economic performance for most applications and, in this particular case, the heat integrated configurations have similar performance as the CDiC. Furthermore, this example illustrates the importance of considering multiple alternative configurations rather than only benchmarking the HIDiC against the CDiC. However, the results are strongly dependent on the economic model for the equipment cost and the utility prices, which are dynamic, regional and highly depend on the possibility for integration with other processing units.

The Guthrie Modular method provides additional information on the cost contribution of each of the equipment types for the distillation columns, that is, columns, tray stacks, heat exchangers, and compressors. These contributions of the individual equipment are illustrated in Figure 6. The dominating expense for the MVRC, the HIDiC and the SIHIDiC is the compressor, whereas the installation of 20 internal heat exchangers is of similar magnitude as the compressor cost in

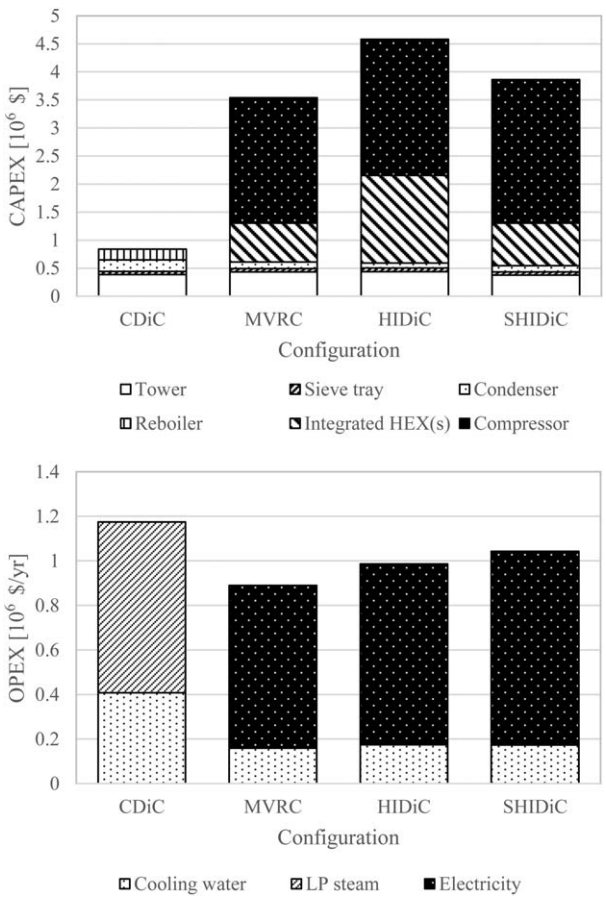

Figure 6. Breakdown of costs associated with the three considered distillation column configurations.

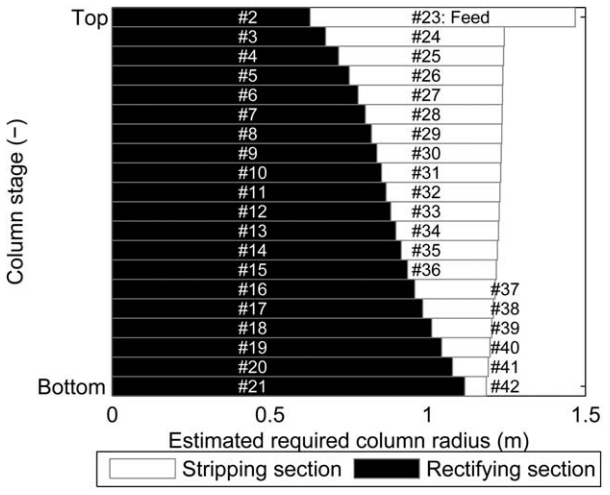

Figure 7. Estimation of column area based on conventional methods with flooding factor of 80% for the HIDiC, demonstrating suitability of the concentric arrangement of the two column sections.

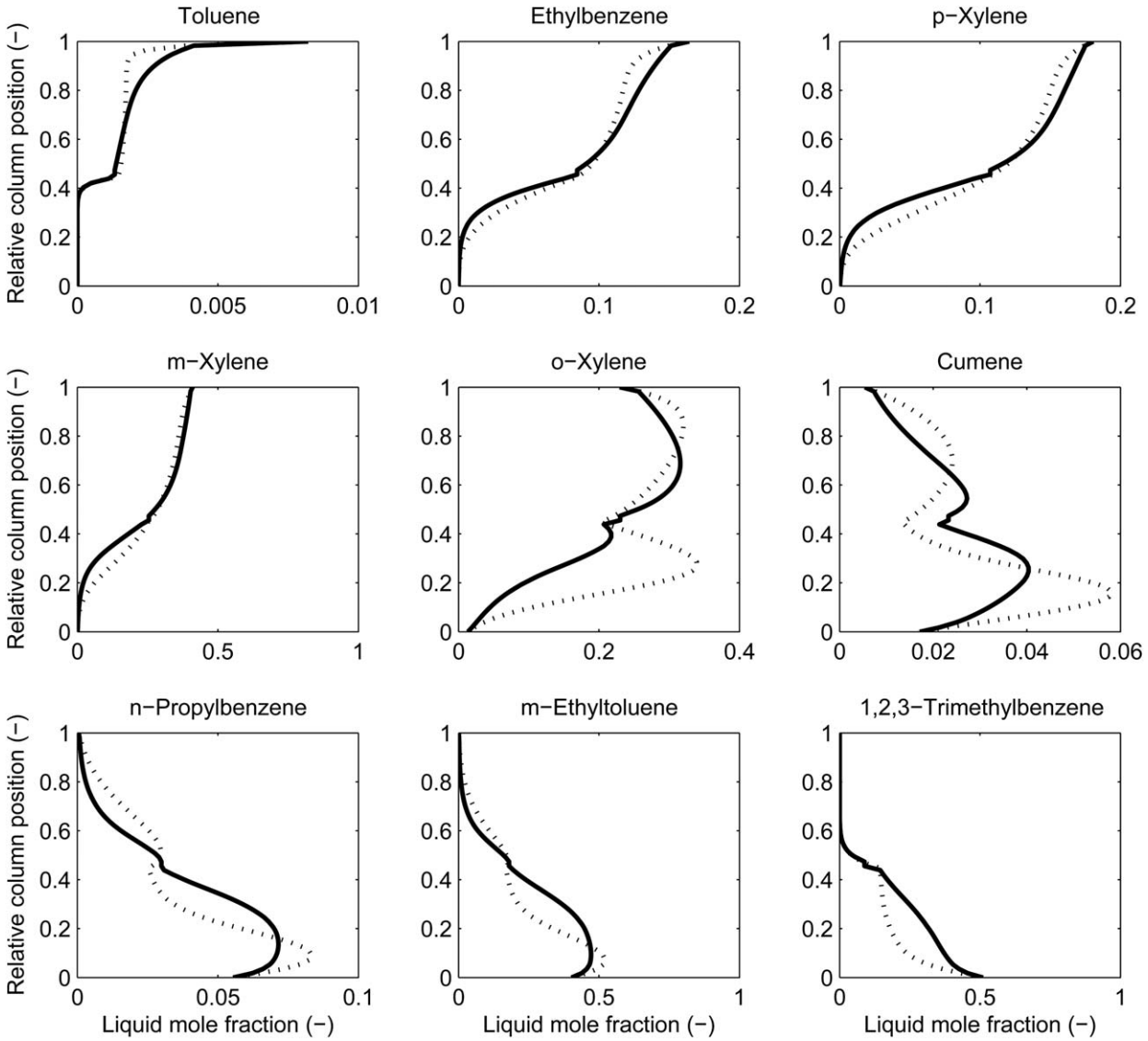

Figure 8. Difference in liquid mole fractions of selected components in simulations of a HIDiC (solid lines) and a CDiC (dashed lines).

the HIDiC. The cost of internal heat exchangers have been halved in the SIHIDiC compared to the HIDiC and the physical realization has been simplified significantly. In terms of OPEX, the HIDiC operates at a lower compression ratio but a higher vapor throughput in the compressor and therefore the higher electricity cost compared to the MVRC. In all the heat-integrated configurations, the gain from investing electrical energy is larger than the economic loss from the more expensive electricity, which is clear by comparing the steam supply cost from the CDiC to electricity costs of the heat-integrated configurations. All heat-integrated configurations reduce energy consumption significantly.

Taking a closer look at the physical realization of internal heat exchange equipment in the "standard" HIDiC, one can estimate the required area for each column stage based on the steady-state flow profiles. Simulation show that a feasible column layout is obtained by adopting the concentric arrangement[34] having the high pressure rectifying section as the inner shell and the stripping section as the outer shell. The sum of the required column area of the two sections is roughly constant, and the obtained radii of the shells are illustrated in Figure 7. In this way, the height of the distillation column can presumably be reduced from 40 trays in the CDiC to 20 trays in the HIDiC, since the HIDiC can contain two adjacent trays in the same column height. In general, reduced equipment height is a desired property of intensifying processes and might contribute to the decision on the best configuration.

Multicomponent separations

The presented model also allows consideration of for multicomponent mixtures. This section presents simulation of a HIDiC for a nine-component mixture consisting of toluene (0.5%), ethylbenzene (10%) p-Xylene (11%) m-Xylene (25%) o-Xylene (14.5%), cumene (1%), n-propylbenzene (2.2%), m-ethyltoluene (15.8%), and 1,2,3-trimethylbenzene (20%), all in mole fractions. Simulation of this separation for a slightly modified and patented version of the HIDiC is provided by Wakabayashi and Hasebe.[35] A feed of 0.0556 mol/s of saturated liquid mixture at 101 kPa is to be separated such the distillate contains no more than 0.7% C9 aromatics and the bottoms contains no more than 1.5% C8 aromatics. The stripping section is operated at 101 kPa, a compression ratio of 2.11 is used and an internal heat-transfer area of 23.2 m^2/stage is installed. In addition, a tray pressure drop of 0.22 kPa is

Table 6. Comparison of Required HIDiC Specifications for Dynamic Simulations Using Different Models

	Presented Model		Liu and Qian Model	
Liquid hydraulics	Weir height, H_W	100 mm	Tray hold-up	3.9 kmol
	Liquid height over weir, H_{oW}	10 mm	Condenser hold-up	16 kmol
	Tray area, A_t (set to 90% of column area)	3.3 m^2	Reboiler hold-up	12 kmol
	Accumulator time constant, τ_{acc}	5 min	Tray time constant[a], τ	60 s
Vapor hydraulics	Pressure drop, ΔP	0.35 kPa	–	–
Compressor	Compressor time constant, τ_{cpr}	10 s	–	–

[a]For tray hydraulics

considered. The studied configurations have 30 stages in the rectifying section and 25 stages in the stripping section. Rigorous simulation yields a 30% reduction in OPEX of a HIDiC compared to a CDiC at a cost of a 381% increase in CAPEX, resulting in a reduction in TAC of 9%. The main investment expense is the 800 kW compressor. One challenge arising from basing HIDiC design on CDiC design is the significant change in the composition profiles inside the column as illustrated in Figure 8.

HIDiC dynamics

The dynamic performance of a HIDiC has been studied extensively in literature through open-loop response analysis, controllability analysis, and controller evaluation studies. However, no models known to us offers manipulation of the power input to the compressor as an indirect way to manipulate the pressure difference of the column sections.

The specification of the dynamic model parameters is performed as suggested in Table 4. The resulting parameters along with equivalent parameters in the simpler Liu and Qian[4] model are provided in Table 6. The equivalent physical and dynamic parameters are based on simulation results of the proposed model. By carrying out dynamic analysis, it was found, that it is feasible to control the stripping section using the condenser duty as manipulated variable and the rectifying section pressure using the compressor duty as manipulated variable. In addition, the reflux drum hold-up and reboiler hold-up were controlled by distillate and bottoms flow rates, respectively. This control strategy was implemented using a discrete time domain with a sampling time of 1 min, thereby closely resembling a continuous time simulation. Three models are

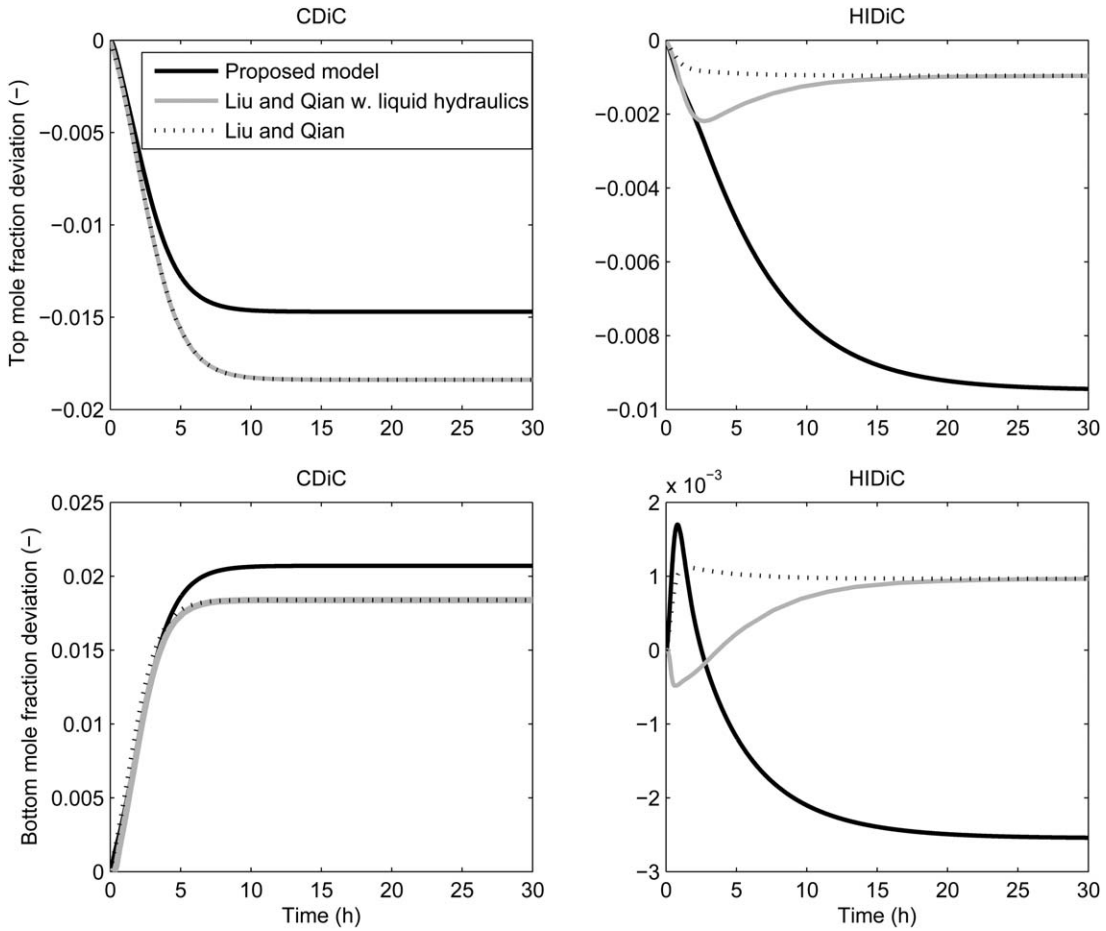

Figure 9. Top and bottom composition dynamic responses for HIDiC subjected to a +5% step change in feed flow rate for three different dynamic models.

considered: The presented model, the model by Liu and Qian, and the Liu and Qian model accounting for linearized tray hydraulics. The linearized tray hydraulics are proposed by Skogestad and Morari[36] for CDiCs. The separation is identical to the separation of benzene/toluene presented in benchmarking study.

Figure 9 illustrates comparisons of dynamic composition responses for three different models and different configurations (CDiC and HIDiC) to a feed +5% step change. It can be seen, that the responses of the CDiC roughly agree for the three different models as expected. The explanation of the responses to an increase in the feed flow rate is as follows. An increased flow rate of partly vaporized feed causes both the distillate and the bottoms compositions to approach that of the feed composition, that is, the mole fraction of the light component decreases in top and increases in bottoms. Comparing the resulting responses from the models for the HIDiC, three fundamentally different responses occurs. First, adding linearized tray hydraulics to the simple model adds numerator dynamics to the HIDiC responses and even an inverse response for the bottom composition. Furthermore, the dominant time constant for the HIDiC appears to be significantly larger for the rigorous model, and the new steady states are inherently different which suggests the modeling of internal heat-transfer accounts for this. For the HIDiC, one additional, opposing effect occurs caused by an increased amount of internal heat transfer. This is a result of an increasing temperature in the rectifying section and a decreasing temperature in the stripping section. This effect is predicted to be more significant and slower using the proposed model.

Discussion

One significant limitation of the presented model is that it is based on equilibrium-stages, resembling those in plate columns. In certain separations, packed column internals are preferred, such as in the structured-HIDiC.[2] Modeling of these configurations requires alternative, rate-based approaches. However, for benchmarking studies without further detailed information of the layout of the column internals, it is reasonable to consider plate columns. In addition, equilibrium-based models are typically preferred because of the smaller number of required model parameters. Another limitation of the presented model is the ideal gas assumption and negligible vapor hold-up.[3] Apart from simplifications of the form of the thermodynamic equations, these assumptions enable modeling of variable stage pressures of nonideal mixtures without increasing model complexity substantially since an ODE system is maintained. This simplifies dynamic simulations. In addition, in the heat-integrated distillation configurations, the compression ratios rarely exceed four due to the costs associated with the compressor, and hence the column operating pressures typically fall within the ideal gas range. However, appropriate terms accounting for vapor phase non-ideality can be included for steady-state simulations if necessary for special applications where the ideal gas assumption does not apply, for example, high-pressure separations or dimerizing gases.

As discussed in relation to step 4 in Figure 4, the selection of design variables for the HIDiC is a more complicated task compared to the CDiC because of an increased number of design degrees of freedom. Hence, there is a need for robust design methods for the HIDiC. The proposed model can provide the simulation tools necessary to aid the development of such design methods.

As mentioned in benchmarking case study, the evaluation of the technoeconomic feasibility of the HIDiC is not a straightforward task. In fact, great uncertainty is associated with this task. Since the HIDiC was introduced in 1977[28] a major concern has been to demonstrate the energetic benefit compared to conventional distillation by either comparing utility consumptions or second-law efficiencies. A more direct measure of the economic feasibility is TAC. TAC calculation, however, relies heavily on the selected economic model. As illustrated by the benzene/toluene separation the installation of internal heat exchangers and a compressor appear to be the major expenses in the HIDiC. Hence, the costing procedures of these units, for example, selection of types of internal heat exchangers will have a significant impact on the TAC. Some authors[37,38] add an additional penalty in the magnitude of 20–50% on the HIDiC capital expenditures to account for increased complexity of the column layout. It is thus vital, that more research is carried out to improve the accuracy of the costing procedure of the HIDiC. Furthermore, the estimation of operation expenditures depends on the utility prices and availability. For example, steam prices might be significantly lower if steam is present in excess in the process or at neighboring facilities. Hence, it is essential to use identical costing scenarios in benchmark studies, which is made possible within the provided framework. It should be noted, that the installation of internal heat transfer does not only affect the economic feasibility but also the technical feasibility since these might reduce the separation performance.

Finally, a crucial element in obtaining technical feasibility is to ensure a stable operation. The HIDiC Dynamics case study illustrates the need for considering models that are more detailed for this purpose, since fundamentally different dynamic behaviors are obtained from the proposed model compared to a simple mass balance model. Furthermore, the proposed model provides a basis for establishing a feasible control scheme that might closely resemble that of an actual process since all actuators are considered.

Conclusions

A generic distillation column model is presented and demonstrated. It can describe both adiabatic and diabatic distillation columns covering among others the conventional, the heat-integrated, and the mechanical vapor recompression distillation column. In addition, the framework offers flexibility to extensions of the current configuration libraries due to the generic structure. The model is embedded in a framework enabling studies to gain insights into, for example, static properties and the dynamic behaviors in a consistent manner. It was shown that the mechanical vapor recompression column outperforms the HIDiC in terms of utility consumption, energy efficiency, and TAC for the separation of benzene/toluene. Dynamic composition responses to feed changes for different dynamic models were investigated and significant changes in the dynamic behavior of the HIDiC were observed.

Notation

A_{ihx} = internal heat exchange area, m^2
A_t = active tray area, m^2
b = availability function, kJ/mol
c_P = constant pressure heat capacity, kJ/mol/K
d = column diameter, m
E = electrical energy flow, kW
F = feed flow rate, mol/s
g = gravitation constant, m/s^2

h = enthalpy, kJ/mol
H = height, m
l = column length, m
L = liquid flow rate, mol/s
M = molar holdup, mol
MW = molecular weight, kg/mol
N = number (integer)
P = pressure, kPa
P^{sat} = saturated pressure, kPa
Q = heat-transfer rate, kW
q = internal heat transfer, kW
R = universal gas constant, kJ/mol/K
s = entropy, kJ/mol/K
S = price, \$/unit
t = time, s
T = temperature, K
T_s = temperature of sink/source, K
T_σ = temperature of surroundings, K
u = internal energy, kJ/mol
U = liquid side stream flow rate, mol/s
U_{ihx} = overall heat-transfer coefficient, kW/m^2/K
v = molar volume, m^3/mol
V = vapor flow rate, mol/s
W = vapor side stream flow rate, mol/s
W_{lost} = lost work, kW
W_{min} = minimum work, kW
x = liquid mole fraction
y = vapor mole fraction
z = feed mole fraction

Greek symbols

Δh_{vap} = heat of vaporization, kJ/mol
ΔP = pressure drop, kPa
η = efficiency
γ = activity coefficient
κ = isentropic expansion factor
ρ = density, kg/m^3

Abbreviations

cnd = condenser
cpr = compressor
CAPEX = capital expenditures
ihx = internal heat exchange
OPEX = operating expenditures
rbl = reboiler
TAC = total annualized cost

Literature Cited

1. Seader JD, Henley EJ, Roper DK. *Separation Process Principles*, 3rd ed. USA: Wiley, 2010.
2. Bruinsma OSL., Krikken T, Cot J, Sarić M, Tromp SA, Olujić Ž, Stankiewicz AI. The structured heat integrated distillation column. *Chem Eng Res Des*. 2012;90:458–470.
3. Skogestad S. Dynamics and control of distillation columns—a critical survey. *Model Identif Control*. 1997;18:177–217.
4. Liu X, Qian J. Modeling, control, and optimization of ideal internal thermally coupled distillation columns. *Chem Eng Technol*. 2000;23:235–241.
5. Ho T, Huang C, Lin J, Lee L. Dynamic simulation for internally heat-integrated distillation columns (HIDiC) for propylene-propane system. *Comput Chem Eng*. 2009;33:1187–1201.
6. Wang L, Makita H, Kano M, Hasebe S. Dynamic start-up model of heat integrated distillation column. *PSE ASIA 2007*. Xi'an, China, 2007.
7. Gani R, Ruiz CA, Cameron IT. A generalized model for distillation columns-I: model description and applications. *Comput Chem Eng*. 1986;10:181–198.
8. Cameron IT, Ruiz CA, Gani R. A generalized model for distillation columns-II: numerical and computational aspects. *Comput Chem Eng*. 1986;10:199–211.
9. Ruiz CA, Cameron IT, Gani R. A generalized dynamic model for distillation columns-III. Study of startup operations. *Comput Chem Eng*. 1988;12:1–14.
10. Gross F, Baumann E, Geser A, Rippin DWT, Lang L. Modelling, simulation and controllability analysis of an industrial heat-integrated distillation process. *Comput Chem Eng*. 1998;22:223–237.
11. Harwardt A, Kraemer K, Marquardt W. Identifying optimal mixture properties for HIDiC application. *Distillation and Absorption*. Eindhoven, The Netherlands, 2010:55–60.
12. Harwardt A, Marquardt W. Heat-integrated distillation columns: vapor recompression or internal heat integration? *AIChE J*. 2012;58:3740–3750.
13. Shenvi AA, Herron DM, Agrawal R. Energy efficiency limitations of the conventional heat integrated distillation column (HIDiC) configuration for binary distillation. *Ind Eng Chem Res*. 2011;50:119–130.
14. Suphanit B. Optimal heat distribution in the internally heat-integrated distillation column (HIDiC). *Energy*. 2011;36:4171–4181.
15. Gutiérrez-Guerra R, Murrieta-Dueñas R, Cortez-González J, Segovia-Hernández JG, Hernández S, Hernández-Aguirre A. Design and optimization of HIDiC distillation columns using a Boltzmann-based estimation of distribution algorithm: influence of volatility. *Distillation and Absorption*. Friedrichshafen, Germany, 2014:655–660.
16. Huang K, Wang S, Iwakabe K, Shan L, Zhu Q. Temperature control of an ideal heat-integrated distillation column (HIDiC). *Chem Eng Sci*. 2007;62:6486–6491.
17. Naito K, Nakaiwa M, Huang K, Endo A, Aso K, Nakanishi T, Nakamura T, Noda H, Takamatsu T. Operation of a bench-scale ideal heat integrated distillation column (HIDiC): an experimental study. *Comput Chem Eng*. 2000;24:495–499.
18. Jiang W, Khan J, Dougal RA. Dynamic centrifugal compressor model for system simulation. *J Power Sour*. 2006;158:1333–1343.
19. Smith JM, Van Ness HC. *Introduction to Chemical Engineering Thermodynamics*, *4th ed*. Singapore: McGraw-Hill, 1986.
20. Fredenslund AA, Gmehling J, Rasmussen P. *Vapor-Liquid Equilibrium Using UNIFAC. A Contribution Method*, *1st ed*. New York: Elsevier, 1977.
21. Wittgens B, Skogestad S. Evaluation of dynamic models of distillation columns with emphasis on the initial response. *Model Identif Control*. 2000;21:83–103.
22. Kolodzie Jr. PA, van Winkle M. Discharge coefficienfts through perforated plates. *AIChE J*. 1957;3:305–312.
23. Fitzmorris RE, Mah RSH. Improving distillation column design using thermodynamic availability analysis. *AIChE J*. 1980;26:265–273.
24. Biegler LT, Grossmann IE, Westerberg AW. *Systematic Methods of Chemical Process Design*, *1st ed*. New Jersey: Prentice-Hall, 1999.
25. Economic indicators. *Chem Eng*. 2013;120:72.
26. Gadalla M, Jiménez L, Olujic Z, Jansens PJ. A thermo-hydraulic approach to conceptual design of an internally heat-integrated distillation column (i-HIDiC). *Comput Chem Eng*. 2007;31:1346–1354.
27. Wakabayashi T, Hasebe S. Higher energy saving with new heat integration arrangement in heat integrated distillation column (HIDiC). *Distillation and Absorption*. Friedrichshafen, Germany, 2014:57–62.
28. Mah RSH, Nicholas JJ Jr., Wodnik RB. Distillation with secondary reflux and vaporization: a comparative evaluation. *AIChE J*. 1977;23:651–658.
29. Nakaiwa M., Huang K, Owa M, Akiya T, Nakane T, Sato M, Takamatsu T. Characteristics of energy savings in an ideal heat-integrated distillation column (HIDiC). *Energy Conversion Engineering Conference*. Honolulu, HI, 1997:1587–1591.
30. Henley EJ, Seader JD. *Equilibrium-Stage Separation Operations in Chemical Engineering*, *1st ed*. USA: Wiley, 1981.
31. Chen H, Huang K, Wang S. A novel simplified configuration for an ideal heat-integrated distillation column (ideal HIDiC). *Sep Purif Technol*. 2010;73:230–242.
32. Ulrich GD, Vasudevan PT. How to estimate utility costs. *Chem Eng*. 2006;113:66.
33. de Rijke A. *Development of a Concentric Internally Heat Integrated Distillation Column (HIDiC)*. Enschede, The Netherlands: Gildeprint Drukkerijen, 2007.
34. Govind R. US Patent 4,681,661, 1987.
35. Wakabayashi T, Hasebe S. Design of heat integrated distillation column by using H-xy and T-xy diagrams. *Comput Chem Eng*. 2013;56:174–183.
36. Skogestad S, Morari M. Understanding the dynamic behavior of distillation columns. *Ind Eng Chem Res*. 1988;27:1848–1862.
37. Nakaiwa M, Huang K, Endo A, Ohmori T, Akiya T, Takamatsu T. Internally heat-integrated distillation columns: a review. *Chem Eng Res Des*. 2003;81:162–177.
38. Olujić Ž, Sun L, de Rijke A, Jansens PJ. Conceptual design of an internally heat integrated propylene-propane splitter. *Energy*. 2006; 31: 3083–3096.

Manuscript received Mar. 13, 2015, and revision received July 8, 2015.